

Navigation System Design Using Time-Varying Complementary Filters

A. PASCOAL

Instituto Superior Técnico

I. KAMINER

U.S. Naval Postgraduate School

P. OLIVEIRA

Instituto Superior Técnico
Portugal

A new methodology for the design of navigation systems for autonomous vehicles is introduced. Using simple kinematic relationships, the problem of estimating the velocity and position of an autonomous vehicle is solved by resorting to special bilinear time-varying filters. These are the natural generalization of linear time-invariant complementary filters that are commonly used to properly merge sensor information available at low frequency with that available in the complementary region. Complementary filters lend themselves to frequency domain interpretations that provide valuable insight into the filtering design process. This work extends these properties to the time-varying setting by resorting to the theory of linear differential inclusions and by converting the problem of weighted filter performance analysis into that of determining the feasibility of a related set of linear matrix inequalities (LMIs). Using this set-up, the stability of the resulting filters as well as their “frequency-like” performance can be assessed using efficient numerical analysis tools that borrow from convex optimization techniques. The mathematical background that is required for complementary time-varying filter analysis and design is introduced. Its application to the design of a navigation system that estimates position and velocity of an autonomous vehicle by complementing position information available from GPS with the velocity information provided by a Doppler sonar system is described.

Manuscript received September 24, 1998; revised November 4, 1999; released for publication July 27, 2000.

IEEE Log No. T-AES/36/4/11359.

Refereeing of this contribution was handled by X. R. Li.

This work was supported by the Office of Naval Research under Contract N0001497AF00002. A Pascoal was also supported by a NATO Fellowship during his 1996-98 sabbatical leave at the NPS and by MAST-III Program of the EC under Contract MAS3-CT97-0092.

Authors' current addresses: A. Pascoal and P. Oliveira, Institute for Systems and Robotics and Department of Electrical Engineering, Instituto Superior Técnico, Av. Rovisco Pais, 1096 Lisboa Codex, Portugal; I. Kaminer, Naval Postgraduate School, Dept. of Aeronautics and Astronautics, Monterey, CA 93943.

U.S. Government work not protected by U.S. copyright.

0018-9251/00/\$10.00 2000 IEEE

I. INTRODUCTION

Currently, there is considerable interest in the development of navigation systems to provide robotic vehicles with the capability to perform complex missions in an autonomous mode. See [1, 4, 15, 16, 18, 21] and the references therein for in-depth presentations of navigation systems for aircraft and [8, 13, 22, 24] for an overview of similar systems and related research issues in the underwater robotics area.

Traditionally, navigation system design is done in a stochastic setting using Kalman–Bucy filtering theory [6]. In the case of nonlinear systems, design solutions are usually sought by resorting to extended Kalman filtering techniques [6]. The stochastic setting requires a complete characterization of process and observation noises, a task that may be difficult, costly, or not suited to the problem at hand. This issue is argued at great length in [7], where the author points out that in a great number of practical applications the filter design process is entirely dominated by constraints that are naturally imposed by the sensor bandwidths. In this case, a design method that explicitly addresses the problem of merging information provided by a given sensor suite over distinct, yet complementary frequency regions is warranted.

Complementary filters have been developed to address this issue explicitly. See for example [7, 18] for a concise introduction to complementary filters and their applications. In the linear time-invariant setting, filter design is ultimately reduced to the problem of decomposing an identity operator into stable low and high pass transfer functions that operate on complementary sensor information. The bandwidth of the low pass transfer function becomes a tuning parameter aimed at matching the physical characteristics of the “low frequency” sensor. Therefore, the emphasis is shifted from a stochastic to a deterministic framework, where the main objective is to shape the filter closed-transfer functions.

This work extends complementary filter design and analysis techniques to a time-varying setting, and offers a solution to the problem of estimating the linear position and velocity of a vehicle using time-varying complementary filters. The time-dependence is imposed by the fact that some of the sensors provide measurements in inertial coordinates, while other measurements are naturally expressed in body axis. To merge the information from both types of sensors (while being able to compensate for sensor biases) requires that the rotation matrix from inertial to body axis be explicitly included in the navigation filters. The resulting filters are bilinear and time varying, but the time-dependence is well structured. By exploiting this structure, the problem of filter design and analysis can be converted into that of determining the feasibility of a set of linear matrix inequalities (LMIs) [3, 20] that arise

in the theory of linear differential inclusions [2, 3]. As a consequence, the stability of the resulting filters as well as their frequency-like performance can be assessed using efficient numerical analysis tools that borrow from convex optimization techniques [3, 17].

Section II reviews some basic mathematical background on linear time-varying systems, induced operator norms, and polytopic systems. Section III sets the motivation for the sections that follow: a simple filtering problem is formulated, and its solution in terms of complementary linear time-invariant filters is described. The new concepts of low and high pass filters for linear time-varying systems are also introduced. Section IV describes the navigation problem addressed here and formulates it mathematically in terms of an equivalent time-varying filter design problem. Section V provides the main theoretical tools for linear time-varying filter design and analysis using the theory of LMIs. Section VI describes a practical algorithm for complementary filter design and illustrates the performance of the new filtering structure in simulation. Section VII discussed extension of the results reported in previous sections to the case of accelerometers. Section VIII discusses implementation issues, and Section IX provides conclusions.

II. MATHEMATICAL BACKGROUND

This section summarizes the mathematical formalism that is required for the study of linear systems, both from an internal and an input-output point of view. The notation is standard; see [11].

Let \mathcal{G} be a stable linear time-invariant (LTI) system with a minimal realization $\Sigma_{\mathcal{G}} := \{A, B, C, D\}$, and let $G(s) = C(sI - A)^{-1}B + D$ denote the corresponding transfer matrix. Then, the induced operator norm $\|\mathcal{G}\|$ equals the \mathcal{H}_{∞} norm of G , denoted $\|G\|_{\infty}$, where

$$\|G\|_{\infty} := \sup_{\omega \in \mathcal{R}} \sigma_{\max}(G^T(-j\omega)G(j\omega))$$

and $\sigma_{\max}(\cdot)$ denotes the maximum singular value of a matrix. Given a positive integer $\gamma > 0$, then $\|\mathcal{G}\| < \gamma$ if and only if there exists a positive definite matrix P that satisfies the matrix inequality [3]

$$\begin{bmatrix} A^T P + PA & PB & C^T \\ B^T P & -\gamma^2 I & D^T \\ C & D & -I \end{bmatrix} < 0. \quad (1)$$

If $D = 0$, then the inequality degenerates to

$$\begin{bmatrix} A^T P + PA + C^T C & PB \\ B^T P & -\gamma^2 I \end{bmatrix} < 0. \quad (2)$$

The above matrix inequalities are LMIs in the matrix variable P . Checking for the existence of $P > 0$ is easily done by resorting to widely available

numerical algorithms [17]. Here we also deal with linear time-varying systems with realizations

$$\begin{aligned} \{A(t), B(t), C(t), D(t)\} &\in \Omega \\ &:= \mathbf{Co}\{\{A_1, B_1, C_1, D_1\}, \dots, \{A_L, B_L, C_L, D_L\}\} \end{aligned}$$

where

$$\mathbf{Co}S := \left\{ \sum_{i=1}^L \lambda_i A_i \mid A_i \in S, \lambda_1 + \dots + \lambda_L = 1 \right\}$$

is the convex hull of the set $S := \{A_1, \dots, A_n\}$. These systems are usually referred to in the literature as *polytopic differential inclusions* [3]. It can be shown that given a polytopic system \mathcal{G} , then $\|\mathcal{G}\| < \gamma$ if there exists a positive definite matrix P such that

$$\begin{bmatrix} A_i^T P + PA_i & PB_i & C_i^T \\ B_i^T P & -\gamma^2 I & D_i^T \\ C_i & D_i & -I \end{bmatrix} < 0; \quad i = 1, 2, \dots, L. \quad (3)$$

Again, checking that such a P exists can be done quite efficiently using highly efficient numerical algorithms.

The results above have their natural counterpart for the case of operators that map L_{∞} to L_{∞} . As discussed in [20], the problem of computing the L_{∞} -induced norm of an operator can still be cast in the framework of LMI theory. However, the computational procedure is more complex and requires a line search over a real parameter.

III. COMPLEMENTARY FILTERS. LOW AND HIGH PASS TIME-VARYING FILTERS

This section reviews the basic structure of complementary filters and introduces the key definitions of low and high pass filters for linear time-varying systems.

A. Complementary Filters: Basic Concepts and Definitions

Complementary filters arise naturally in the context of signal estimation based on measurements provided by sensors over distinct, yet complementary regions of frequency. Brown [7] was the first author to stress the importance of complementary filters in navigation system design. Since then, this subject has been studied in a number of publication that address theoretical as well as practical implementation issues; see for example [1, 16, 18, 19, 21] and the references therein. The key ideas in complementary filtering are very intuitive, and can be simply introduced by referring to the example of Fig. 1. The figure captures the practical situation where it is required to estimate the heading ψ of a vehicle based on measurements r_m and ψ_m of $r = \psi$ and ψ , respectively, provided by a

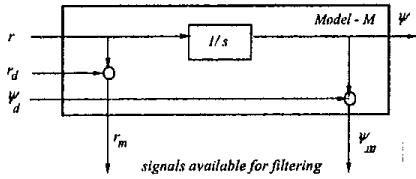


Fig. 1. Process model.

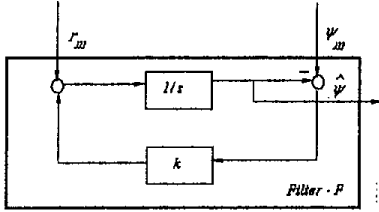


Fig. 2. Complementary filter.

rate gyro and a fluxgate compass. The measurements are corrupted by disturbances r_d and ψ_d .

Let $\psi(s)$ and $r(s)$ denote the Laplace transforms of ψ and r , respectively. Then, for every $k > 0$, $\psi(s)$ admits the stable decomposition

$$\begin{aligned} \psi(s) &= \frac{s+k}{s+k} \psi(s) = \frac{k}{s+k} \psi(s) + \frac{s}{s+k} \psi(s) \\ &= T_1(s) \psi(s) + T_2(s) \psi(s) \end{aligned} \quad (4)$$

where $T_1(s) = k/(s+k)$ and $T_2(s) = s/(s+k)$ satisfy the equality

$$T_1(s) + T_2(s) = I. \quad (5)$$

Using the relationship $r(s) = s\psi(s)$, it follows from the above equations that

$$\psi(s) = F_\psi(s) \psi(s) + F_r(s) r(s)$$

where $F_\psi(s) = T_1(s) = k/(s+k)$ and $F_r(s) = 1/(s+k)$. This suggests a filter with the structure

$$\hat{\psi} = \mathcal{F}_\psi \psi_m + \mathcal{F}_r r_m$$

where \mathcal{F}_ψ and \mathcal{F}_r are LTI operators with transfer functions $F_\psi(s)$ and $F_r(s)$, respectively. Clearly, the filter admits the state space realization

$$\begin{aligned} \dot{\hat{\psi}} &= -k\hat{\psi} + k\psi_m + r_m \\ &= r_m + k(\psi_m - \hat{\psi}) \end{aligned} \quad (6)$$

that is represented in Fig. 2.

Let \mathcal{T}_1 and \mathcal{T}_2 denote LTI operators with transfer functions $T_1(s)$ and $T_2(s)$, respectively. Simple computations show that

$$\hat{\psi} = (\mathcal{T}_1 + \mathcal{T}_2)\psi + \mathcal{F}_\psi \psi_d + \mathcal{F}_r r_d$$

that is, the estimate $\hat{\psi}$ consists of an undistorted copy $(\mathcal{T}_1 + \mathcal{T}_2)\psi = \psi$ of the original signal ψ , together with corrupting terms that depend on the measurement disturbances ψ_d and r_d .

Notice the following important properties.

1) $T_1(s)$ is low pass. The filter relies on the information provided by the compass at low frequency only.

2) $T_2(s) = I - T_1(s)$. The filter blends the information provided by the compass in the low frequency region with that available from the rate gyro in the complementary region.

3) The break frequency is simply determined by the choice of the parameter k .

The frequency decomposition induced by the complementary filter structure holds the key to its practical success, since it mimicks the natural frequency decomposition induced by the physical nature of the sensors themselves. Compasses provide reliable information at low frequency only, whereas rate gyros exhibit biases and drift phenomena in the same frequency region and are therefore useful at higher frequencies.

Complementary filter design is then reduced to the computation of the gain k so as to meet a target break frequency that is entirely dictated by the physical characteristics of the sensors. From this point of view, the emphasis is shifted from a stochastic framework that relies heavily on a correct description of process and measurement noise [7] and the minimization of filter errors-to a deterministic framework that aims at shaping the filter closed-loop functions.

As convincingly argued in [7], the latter approach is best suited to tackle a large number of practical situations where the characterization of process and measurement disturbances in a stochastic context does not fit the problem at hand, the filter design process being entirely dominated by the constraints imposed by sensor bandwidths. Once this set-up is adopted, however, one is free to use any efficient design method, the design parameters being simply viewed as ‘‘tuning knobs’’ to shape the characteristics of the closed-loop operators. In this context, filter design can be done using H_2 or H_∞ design techniques [6, 10–12, 19]. Filter analysis is easily carried out in the frequency domain using Bode plots. In the simple case described here, the underlying process model can be written as

$$\begin{cases} \dot{\psi} = r_m - r_d \\ \psi_m = \psi + \psi_d \end{cases} \quad (7)$$

where r_d and ψ_d play the roles of process and measurement disturbances, respectively. Notice the important fact that ψ_m (the measured value of ψ) is an input to the system. In an H_2 setting, the objective is to minimize the estimation error $\psi - \hat{\psi}$ for given values of the covariances of ψ_d and r_d . The optimal solution to this problem has the complementary filter structure described in (6). The covariances of ψ_d and r_d are simply viewed as design parameters to vary the break frequency.

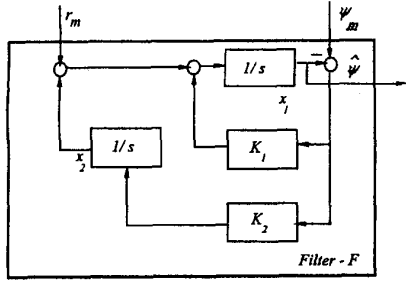


Fig. 3. Complementary filter with bias estimation.

In practice, the simple complementary structure described above can be modified to meet additional constraints. For example, to achieve steady state rejection of the rate gyro bias, the filter must be augmented with an integrator to obtain the new complementary filter depicted in Fig. 3 with the realization

$$\begin{aligned} \begin{bmatrix} \dot{x}_1 \\ \dot{x}_2 \end{bmatrix} &= \begin{bmatrix} -k_1 & 1 \\ -k_2 & 0 \end{bmatrix} \begin{bmatrix} x_1 \\ x_2 \end{bmatrix} + \begin{bmatrix} k_1 \\ k_2 \end{bmatrix} \psi_m + \begin{bmatrix} 1 \\ 0 \end{bmatrix} r_m \\ \hat{\psi} &= [1 \quad 0] \begin{bmatrix} x_1 \\ x_2 \end{bmatrix} \end{aligned} \quad (8)$$

where x_1 and x_2 denote the states associated with $\hat{\psi}$ and the bias term, respectively, and k_1 and k_2 are filter gains. To bring out its relationship with a conventional observer (note Kalman filter is another example of such an observer with the gains selected to minimize a quadratic cost function), the expression above can be rewritten as

$$\begin{cases} \dot{\mathbf{x}} = \mathbf{A}\mathbf{x} + \mathbf{B}u + \mathbf{H}(y - \hat{y}) \\ \hat{y} = \mathbf{C}\mathbf{x} \end{cases} \quad (9)$$

where $\mathbf{x} = [x_1 \ x_2]^T$, $u = r_m$, $y = \psi_m$, and

$$\begin{aligned} \mathbf{A} &= \begin{bmatrix} 0 & 1 \\ 0 & 0 \end{bmatrix}, & \mathbf{B} &= \begin{bmatrix} 1 \\ 0 \end{bmatrix}, \\ \mathbf{C} &= [1 \quad 0], & \mathbf{H} &= \begin{bmatrix} k_1 \\ k_2 \end{bmatrix}. \end{aligned}$$

Simple computations show that in this case

$$\hat{\psi} = (T_1 + T_2)\psi + \eta$$

where

$$T_1(s) = \frac{k_1 s + k_2}{s^2 + k_1 s + k_2}, \quad T_2(s) = \frac{s^2}{s^2 + k_1 s + k_2}$$

and $\eta = \mathcal{F}_\psi \psi_d + \mathcal{F}_r r_d$ is a noise term, the intensity of which depends on $F_\psi(s) = T_1(s)$ and $F_r(s) = s / (s^2 + k_1 s + k_2)$. Again, notice that $T_1(s) + T_2(s) = I$, $T_1(s)$ is low pass, and $T_2(s)$ is high pass. The filter blends naturally the information provided by the compass at low frequency with that available from the rate gyro in the complementary frequency range,

leaving the original signal ψ undistorted. Furthermore, any constant terms in r_d (rate gyro bias) is naturally rejected at the output since $F_r(0) = 0$. Notice also that the filter rejects naturally high frequency noise present in the fluxgate measurements.

In view of the discussion above, we henceforth adopt a deterministic framework for complementary filter design and analysis where the objective is to shape the filter transfer functions to obtain desired bandwidths. Furthermore, in preparation for the sections that follow, it is convenient to formally introduce the definition of a complementary filter for the underlying process model (7) (with $r_d = \psi_d = 0$) in a state-space framework; see Fig. 1.

DEFINITION (r, ψ) Complementary Filter. Consider the process model

$$\mathcal{M}_{\psi r} := \begin{cases} \dot{\psi} = r \\ \psi_m = \psi \\ r_m = r \end{cases} \quad (10)$$

and a filter \mathcal{F} with realization

$$\begin{aligned} \dot{\mathbf{x}} &= \mathbf{A}\mathbf{x} + \mathbf{B}_r r_m + \mathbf{B}_\psi \psi_m \\ \hat{\psi} &= \mathbf{C}\mathbf{x}. \end{aligned}$$

Then, \mathcal{F} is said to be a complementary filter for $\mathcal{M}_{\psi r}$ if

- \mathcal{F} is internally stable,
- for every any initial conditions $\psi(0)$ and $\mathbf{x}(0)$
- $\lim_{t \rightarrow \infty} \{\psi(t) - \hat{\psi}(t)\} = 0$,
- \mathcal{F} satisfies a bias rejection property, that is,
- $\lim_{t \rightarrow \infty} \hat{\psi} = 0$ when $\psi_m = 0$ and r_m is an arbitrary constant,

the operator $\mathcal{F}_\psi : \psi_m \rightarrow \hat{\psi}$ is a finite bandwidth low pass filter.

Clearly, for every $k_1, k_2 > 0$ the filter with realization (8) is a complementary filter for the process $\mathcal{M}_{\psi r}$ in (10). It is important to point out that according to the definition above, (8) is but one representative of a large class of complementary filters for $\mathcal{M}_{\psi r}$. However, in this work, and for simplicity of exposition, we restrict ourselves to complementary filter structures similar to (8).

B. Low and High Pass Filters: Linear Time-Varying Setting

The concepts of low pass and high pass filters play a key role in assessing the performance of complementary filters and are well understood in the case of LTI systems. We now extend these concepts to the class of linear time-varying systems. The new concepts play a major role in assessing the performance of the linear time-varying complementary filters that are introduced later.

DEFINITION Low Pass Property. Let \mathcal{G} be a linear, internally stable time-varying system and let \mathcal{W}_ω^n be a low pass, LTI Chebyshev filter of order n and cutoff frequency ω . The system \mathcal{G} is said to satisfy a low pass property with indices (ϵ, n) over $[0, \omega_c]$ if

$$\|(\mathcal{G} - I)W_\omega^n\| < \epsilon.$$

DEFINITION Low Pass Filter with Bandwidth ω_c . A linear, internally stable time-varying system \mathcal{G} is said to be an (ϵ, n) low pass filter with bandwidth ω_c if

$\lim_{\omega \rightarrow 0} \|(\mathcal{G} - I)W_\omega^n\|$ is well defined and equals 0, $\omega_c := \sup\{\omega : \|(\mathcal{G} - I)W_\omega^n\| < \epsilon\}$, i.e. \mathcal{G} satisfies a low pass property with indices (ϵ, n) over $[0, \omega]$ for all $\omega \in [0, \omega_c)$ but fails to satisfy that property whenever $\omega \geq \omega_c$.

for every $\delta > 0$, there exists $\omega^* = \omega^*(\delta)$ such that $\|\mathcal{G}(I - W_\omega^n)\| < \delta$ for $\omega > \omega^*$.

DEFINITION High Pass Filter with Break Frequency ω_c . A linear, internally stable time-varying system \mathcal{G} is said to be an (ϵ, n) high pass filter with break frequency ω_c if $(I - \mathcal{G})$ is an (ϵ, n) low pass filter with bandwidth ω_c .

The conditions in the definition of low pass filters generalize the following facts that are obvious in the LTI case.

- 1) The filter must provide a gain equal to one at zero frequency.
- 2) There is a finite band of frequencies over which the system behavior replicates very closely that of an identity operator.
- 3) The system gain rolls-off to zero at high frequency.

Notice the role played by the weighting operator \mathcal{W}_ω^n , which was arbitrarily selected as a Chebyshev filter. In practice, the order of the filter can be made sufficiently large so as to make it effectively select the “low frequency components” of the input signal.

IV. NAVIGATION SYSTEM DESIGN. PROBLEM FORMULATION

This section describes the navigation problem that is the main focus of this work and formulates it mathematically in terms of an equivalent filter design problem. For the sake of clarity, we first introduce some basic notation and summarize the kinematic equations for a general vehicle.

A. Notation. Vehicle Kinematics: A Summary

Let $\{\mathcal{I}\}$ be a reference frame, and let $\{\mathcal{B}\}$ denote a body-fixed frame that moves with the vehicle. The following notation is required.

$\mathbf{p} = [x \ y \ z]^T$	Position of the origin of $\{\mathcal{B}\}$ measured in $\{\mathcal{I}\}$.
${}^I\mathbf{v} = [\dot{x} \ \dot{y} \ \dot{z}]^T$	Linear velocity of the origin of $\{\mathcal{B}\}$ measured in $\{\mathcal{I}\}$.
$\mathbf{v} = [u \ v \ w]^T$	Linear velocity of the origin of $\{\mathcal{B}\}$ with respect to $\{\mathcal{I}\}$, resolved in $\{\mathcal{B}\}$.
$\boldsymbol{\omega} = [p \ q \ r]^T$	Angular velocity of $\{\mathcal{B}\}$ with respect to $\{\mathcal{I}\}$, resolved in $\{\mathcal{B}\}$.
$\boldsymbol{\lambda} = [\phi \ \theta \ \psi]^T$	Vector of roll, pitch, and yaw angles that parametrize locally the orientation of frame $\{\mathcal{B}\}$ with respect to $\{\mathcal{I}\}$.

Given two frames $\{\mathcal{A}\}$ and $\{\mathcal{B}\}$, ${}^A_B\mathcal{R}$ denotes the rotation matrix from $\{\mathcal{B}\}$ to $\{\mathcal{A}\}$. In particular, ${}^I_B\mathcal{R}$ (abbreviated \mathcal{R}) is the rotation matrix from $\{\mathcal{B}\}$ to $\{\mathcal{I}\}$, parametrized locally by $\boldsymbol{\lambda}$, that is, $\mathcal{R} = \mathcal{R}(\boldsymbol{\lambda})$. Since \mathcal{R} is a rotation matrix, it satisfies the orthonormality condition $\mathcal{R}^T \mathcal{R} = I$. Given the angular velocity vector $\boldsymbol{\omega}$, then

$$\dot{\boldsymbol{\lambda}} = Q(\boldsymbol{\lambda})\boldsymbol{\omega}$$

where $Q(\boldsymbol{\lambda})$ is a matrix that relates the derivative of $\boldsymbol{\lambda}$ with $\boldsymbol{\omega}$. The following kinematic relations apply [4]:

$$\dot{\mathbf{p}} = {}^I\mathbf{v} = \mathcal{R}\mathbf{v} \quad (11)$$

$$\dot{\mathcal{R}} = \mathcal{R}\mathcal{S}(\boldsymbol{\omega}) \quad (12)$$

where

$$\mathcal{S}(\boldsymbol{\omega}) := \begin{bmatrix} 0 & -\omega_z & \omega_y \\ \omega_z & 0 & -\omega_x \\ -\omega_y & \omega_x & 0 \end{bmatrix} \quad (13)$$

is a skew symmetric matrix, that is, $\mathcal{S}^T = -\mathcal{S}$. The matrix \mathcal{S} satisfies the relationship $\mathcal{S}(a)b = a \times b$, where a, b are arbitrary vectors and \times denotes the cross product operation. Furthermore, $\|\mathcal{S}(\boldsymbol{\omega})\| = \|\boldsymbol{\omega}\|$.

B. Time-Varying Complementary Filters. Navigation Problem Formulation

We now extend the basic concepts of complementary filtering to the time-varying setting. The motivation for this work can be simply described by considering the example where one is interested in estimating the position \mathbf{p} and velocity ${}^I\mathbf{v}$ of a vehicle based on measurements \mathbf{p}_m and \mathbf{v}_m of \mathbf{p} and \mathbf{v} , respectively. In the case of an ocean surface vehicle, \mathbf{p}_m is provided by a Differential Global Positioning System (DGPS), whereas \mathbf{v}_m is provided by a Doppler sonar. In the case of a fully submerged underwater vehicle, \mathbf{p}_m can be provided by a Long Baseline System.

It must be stressed that due to the physical characteristic of the Doppler sonar the measurement \mathbf{v}_m is naturally expressed in body-axis, that is, in

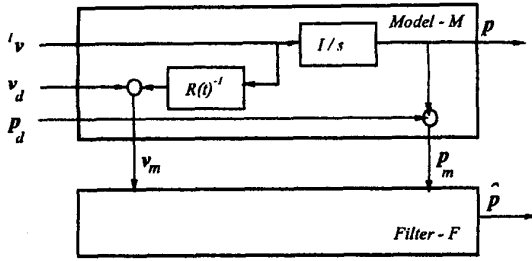


Fig. 4. Process model.

the reference frame $\{B\}$. Furthermore, Doppler bias effects are also naturally expressed in $\{B\}$. This is in contrast with the measurements \mathbf{p}_m , which are directly available in the reference frame $\{I\}$. These facts impose important constraints on the class of complementary filters for position and velocity estimation, as becomes clear later.

The underlying process model \mathcal{M}_{pv} is depicted in Fig. 4, where \mathcal{F} is a dynamical system (filter) that operates on the measurements \mathbf{p}_m and \mathbf{v}_m to provide estimates $\hat{\mathbf{p}}$ of \mathbf{p} . In the figure, \mathbf{p}_d and \mathbf{v}_d are measurement disturbances. As in the last section, we study the situation where $\mathbf{p}_d = 0$ and $\mathbf{v}_d = \mathbf{v}_{d,0}$ where $\mathbf{v}_{d,0}$ is the Doppler bias. This set-up is all that is required for the design of complementary filters from a frequency-like domain point of view. Notice that the process model \mathcal{M}_{pv} is time-varying due to the presence of the rotation matrix $R(t)$. However, the entries of $R(t)$ and their derivatives are not arbitrary functions of time but exhibit bounds that depend on each specific vehicle mission under consideration. For example, if an underwater vehicle motion is restricted to the horizontal plane and the maximum yaw rate achievable with that vehicle is r_{\max} , then this information must be explicitly included in the description of the process model \mathcal{M}_{pv} as we explain below. We now introduce the following definitions.

DEFINITION Process Model \mathcal{M}_{pv} . The process model \mathcal{M}_{pv} is given by

$$\mathcal{M}_{pv} := \begin{cases} \dot{\mathbf{p}} = \mathbf{v} \\ \mathbf{p}_m = \mathbf{p} \\ \mathbf{v}_m = \mathcal{R}^{-1}\mathbf{v} + \mathbf{v}_{d,0}. \end{cases} \quad (14)$$

We further assume that the matrix \mathcal{R} and its derivative $\dot{\mathcal{R}}$ are constrained through the inequalities

$$|\phi(t)| \leq \phi_{\max}, \quad |\theta(t)| \leq \theta_{\max} \quad (15)$$

and

$$|p(t)| \leq p_{\max}, \quad |q(t)| \leq q_{\max}, \quad |r(t)| \leq r_{\max} \quad (16)$$

for all $t \in \mathcal{R}_+$. Notice in the definition above that there are constraints on the roll and pitch angles ϕ and θ , respectively, but not on the yaw angle ψ . This is due to the fact that ocean vehicles are designed to undergo arbitrary maneuvers in yaw, but pitch and roll excursions are restricted by vehicle construction.

DEFINITION Candidate Complementary Filter.

Consider the process model \mathcal{M}_{pv} in (14) with $\mathbf{v}_{d,0}$ an arbitrary constant, and let \mathcal{F} be a linear time-varying filter with realization

$$\mathcal{F} := \begin{cases} \dot{\mathbf{x}} = A(t)\mathbf{x} + B_p(t)\mathbf{p}_m + B_v(t)\mathbf{v}_m \\ \hat{\mathbf{p}} = C(t)\mathbf{x}. \end{cases} \quad (17)$$

Then, \mathcal{F} is said to be a *candidate complementary filter* for \mathcal{M}_{pv} if

- \mathcal{F} is internally stable,
- for every initial conditions $\mathbf{p}(0)$ and $\mathbf{x}(0)$,
- $\lim_{t \rightarrow \infty} \{\mathbf{p}(t) - \hat{\mathbf{p}}(t)\} = 0$,
- \mathcal{F} satisfies a bias rejection property, that is,
- $\lim_{t \rightarrow \infty} \hat{\mathbf{p}} = 0$ when $\mathbf{v} = 0$.

DEFINITION Complementary Filter with Break Frequency ω_c . Let \mathcal{F} be a candidate

complementary filter for \mathcal{M}_{pv} , and let \mathcal{F}_p denote the corresponding operator from \mathbf{p}_m to $\hat{\mathbf{p}}$. Then, \mathcal{F} is said to be an (ϵ, n) *complementary filter* for \mathcal{M}_{pv} with break frequency ω_c if \mathcal{F}_p is an (ϵ, n) *low pass filter* with bandwidth ω_c .

The discussion in the previous sections leads directly to the following filter design problem.

Problem formulation. Given the process model \mathcal{M}_{pv} in (14) and positive numbers ω_c , n , and ϵ , find an (ϵ, n) complementary filter for \mathcal{M}_{pv} with break frequency ω_c .

V. COMPLEMENTARY FILTER DESIGN. MAIN RESULTS

This section introduces a specific candidate complementary filter structure for \mathcal{M}_{pv} and derives sufficient conditions for the existence of a complementary filter with the structure adopted that meets required bandwidth constraints.

A. Candidate Complementary Filter Structure

Fig. 5 depicts the candidate filter structure for \mathcal{M}_{pv} that is adopted here. The structure is motivated by the simple example described in Section III, where an extra integrator was inserted to estimate the rate gyro bias. Notice however that the filter explicitly includes the rotation matrix $\mathcal{R}(t)$, which we assume is available from an attitude reference system. The issue of robust filter performance against uncertainties

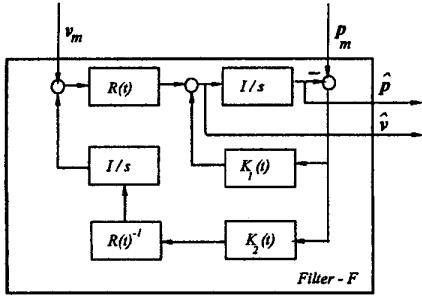


Fig. 5. Complementary filter.

in the measurement of $\mathcal{R}(t)$ is addressed later in this section. In what follows, for simplicity of notation, we often avoid writing the explicit dependence of time-varying matrices on time. The following result is obtained.

THEOREM 1 Consider the process model \mathcal{M}_{pv} and the time-varying filter

$$\mathcal{F} := \begin{cases} \dot{\mathbf{x}}_1 = R\mathbf{v}_m + R\mathbf{x}_2 + K_1(\mathbf{p} - \mathbf{x}_1) \\ \dot{\mathbf{x}}_2 = R^{-1}K_2(\mathbf{p} - \mathbf{x}_1) \\ \hat{\mathbf{p}} = \mathbf{x}_1. \end{cases} \quad (18)$$

Suppose the filter \mathcal{F} is internally stable. Then, \mathcal{F} is a candidate complementary filter for \mathcal{M}_{pv} .

PROOF From the assumptions, the time-varying filter has the realization

$$\mathcal{F} := \left[\begin{array}{c|c} A(t) & [B_p(t) \ B_v(t)] \\ \hline C(t) & 0 \end{array} \right]$$

where

$$A(t) = \begin{bmatrix} -K_1 & R \\ -R^{-1}K_2 & 0 \end{bmatrix}, \quad B_p(t) = \begin{bmatrix} K_1 \\ R^{-1}K_2 \end{bmatrix},$$

$$B_v(t) = \begin{bmatrix} R \\ 0 \end{bmatrix}, \quad C(t) = \begin{bmatrix} I \\ 0 \end{bmatrix}.$$

Furthermore, $\mathbf{v}_m = \mathbf{v} + \mathbf{v}_{d,0}$, where $\mathbf{v}_{d,0}$ is an arbitrary constant vector (Doppler bias). Let $\Phi(t, \tau)$ denote the state transition matrix associated with $A(t)$. Then, using the equalities

$$B_p \mathbf{p}(\tau) = -A(\tau) \begin{bmatrix} \mathbf{p}(\tau) \\ 0 \end{bmatrix},$$

$$B_v \mathbf{v}(\tau) = \begin{bmatrix} \frac{d}{d\tau} \mathbf{p}(\tau) \\ 0 \end{bmatrix},$$

$$B_v \mathbf{v}_{d,0} = -A(\tau) \begin{bmatrix} 0 \\ \mathbf{v}_{d,0} \end{bmatrix}$$

the filter state evolution is given by

$$\begin{aligned} \begin{bmatrix} \mathbf{x}_1(t) \\ \mathbf{x}_2(t) \end{bmatrix} &= \Phi(t, t_0) \begin{bmatrix} \mathbf{x}_1(t_0) \\ \mathbf{x}_2(t_0) \end{bmatrix} \\ &+ \int_{t_0}^t \Phi(t, \tau) \{ B_p \mathbf{p}(\tau) + B_v (\mathbf{v}(\tau) + \mathbf{v}_{d,0}) \} d\tau \\ &= \Phi(t, t_0) \begin{bmatrix} \mathbf{x}_1(t_0) \\ \mathbf{x}_2(t_0) \end{bmatrix} \\ &+ \int_{t_0}^t \Phi(t, \tau) \left\{ -A(\tau) \begin{bmatrix} \mathbf{p}(\tau) \\ 0 \end{bmatrix} + \begin{bmatrix} \frac{d}{d\tau} \mathbf{p}(\tau) \\ 0 \end{bmatrix} \right\} d\tau \\ &+ \int_{t_0}^t \Phi(t, \tau) \left\{ -A(\tau) \begin{bmatrix} 0 \\ \mathbf{v}_{d,0} \end{bmatrix} \right\} d\tau. \end{aligned} \quad (19)$$

The transition matrix $\Phi(t, \tau)$ satisfies

$$\frac{d}{d\tau} \Phi(t, \tau) = -\Phi(t, \tau) A(\tau) \quad (20)$$

and therefore (19) can also be written as

$$\begin{aligned} \begin{bmatrix} \mathbf{x}_1(t) \\ \mathbf{x}_2(t) \end{bmatrix} &= \Phi(t, t_0) \begin{bmatrix} \mathbf{x}_1(t_0) \\ \mathbf{x}_2(t_0) \end{bmatrix} \\ &+ \int_{t_0}^t \left\{ \frac{d}{d\tau} \left(\Phi(t, \tau) \begin{bmatrix} \mathbf{p}(\tau) \\ 0 \end{bmatrix} \right) \right\} d\tau \\ &+ \int_{t_0}^t \left\{ \frac{d}{d\tau} \left(\Phi(t, \tau) \begin{bmatrix} 0 \\ \mathbf{v}_{d,0} \end{bmatrix} \right) \right\} d\tau \\ &= \Phi(t, t_0) \begin{bmatrix} \mathbf{x}_1(t_0) \\ \mathbf{x}_2(t_0) \end{bmatrix} + \begin{bmatrix} \mathbf{p}(t) \\ 0 \end{bmatrix} - \Phi(t, t_0) \begin{bmatrix} \mathbf{p}(t_0) \\ 0 \end{bmatrix} \\ &+ \begin{bmatrix} 0 \\ \mathbf{v}_{d,0} \end{bmatrix} - \Phi(t, t_0) \begin{bmatrix} 0 \\ \mathbf{v}_{d,0} \end{bmatrix}. \end{aligned} \quad (21)$$

Since the filter is stable, $\lim_{t \rightarrow \infty} \|\Phi(t, t_0)\| = 0$. The results follows immediately by observing that $\hat{\mathbf{p}} = \mathbf{x}_1$.

Notice that the state \mathbf{x}_2 of the appended integrator tends asymptotically to $-\mathbf{v}_{d,0}$. Thus, \mathbf{x}_2 provides an estimate of the Doppler bias in the body frame. This result makes perfect sense from a physical point of view since the bias is constant in the body frame (not in the reference frame \mathcal{I}).

B. Candidate Complementary Filter. Sufficient Conditions for Stability and Guaranteed Break Frequency

The next result establishes sufficient conditions for the existence of fixed gains K_1 and K_2 such that the candidate filter is internally stable and has a guaranteed break frequency of at least ω_c , where ω_c is a design parameter. In preparation for that result we let

$$\omega_r = [p_r \ q_r \ r_r]^T := \mathcal{R}\omega$$

and define

$$\mathcal{S}_r := \mathcal{S}(\omega_r) = \dot{\mathcal{S}}(\mathcal{R}\omega).$$

Given the original design bounds (15)–(16), it is possible to compute positive upper bounds p_r^+ , q_r^+ , and r_r^+ such that

$$|p_r| \leq p_r^+, \quad |q_r| \leq q_r^+, \quad |r_r| \leq r_r^+. \quad (22)$$

Let $p_r^- = -p_r^+$, $q_r^- = -q_r^+$, $r_r^- = -r_r^+$ and construct the set $\{\omega_r^i, i = \{1, \dots, 8\}\}$, where

$$\omega_r^1 = \begin{bmatrix} p_r^- \\ q_r^- \\ r_r^- \end{bmatrix}, \quad \omega_r^2 = \begin{bmatrix} p_r^+ \\ q_r^- \\ r_r^- \end{bmatrix}, \quad \omega_r^3 = \begin{bmatrix} p_r^- \\ q_r^+ \\ r_r^- \end{bmatrix},$$

$$\omega_r^4 = \begin{bmatrix} p_r^+ \\ q_r^+ \\ r_r^- \end{bmatrix}, \dots, \omega_r^8 = \begin{bmatrix} p_r^+ \\ q_r^+ \\ r_r^+ \end{bmatrix}.$$

Then

$$\omega_r \in \text{Co}\{\omega_r^i, i = \{1, \dots, 8\}\} \quad \text{and}$$

$$S_r \in \text{Co}\{S_r^i = S(\omega_r^i); i = \{1, \dots, 8\}\}.$$

THEOREM 2 Consider the linear time-varying filter (18) and assume that the bounds (22) on ω_r apply. Given n and ω_c , let

$$\mathcal{W}_{\omega_c}^n := \left[\begin{array}{c|c} A_w & B_w \\ \hline C_w & 0 \end{array} \right]$$

be a minimal realization for the weighting Chebyshev filter introduced in Section IIIB. Further let

$$F = \begin{bmatrix} 0 & I \\ 0 & S_r \end{bmatrix}, \quad H = [-I \quad 0].$$

Suppose that given $\epsilon > 0 \exists K \in \mathcal{R}^{6 \times 3}$, $P \in \mathcal{R}^{(6+n) \times (6+n)}$, $P > 0$, such that the LMIs

$$L_{LR}(K, P, \epsilon) := \left[\begin{array}{c|c} P \left[\begin{array}{cc} F_i + KH & KC_w \\ 0 & A_w \end{array} \right] + \left[\begin{array}{cc} F_i + KH & KC_w \\ 0 & A_w \end{array} \right]^T P & P \begin{bmatrix} 0 \\ B_w \end{bmatrix} \\ \hline \left[\begin{array}{cc} H^T \\ -C_w^T \end{array} \right] [H \quad -C_w] & \\ \hline [0 \quad B_w^T] P & -\epsilon^2 I \end{array} \right] < 0$$

$$F_i = \begin{bmatrix} 0 & I \\ 0 & S(\omega_r^i) \end{bmatrix}, \quad i = \{1, \dots, 8\} \quad (23)$$

are satisfied. Then, the constant gains

$$\begin{bmatrix} K_1 \\ K_2 \end{bmatrix} := K$$

make the filter \mathcal{F} internally stable. Furthermore, the operator $\mathcal{F}_p: \mathbf{p} \rightarrow \hat{\mathbf{p}}$ satisfies a low pass property with indices (ϵ, n) over $[0, \omega_c]$, that is, $\|(\mathcal{F}_p - I)W_{\omega_c}^n\| < \epsilon$.

PROOF Given the realization (18), consider the Lyapunov coordinate transformation [5]

$$\zeta(t) = \bar{P}(t)\mathbf{x}(t)$$

where

$$\bar{P}(t) = \begin{bmatrix} I & 0 \\ 0 & R(t) \end{bmatrix}.$$

With this change of coordinates, the operator \mathcal{F}_p admits the realization

$$\mathcal{F}_p = \begin{cases} \dot{\zeta} = (\bar{P}A\bar{P}^{-1} + \dot{\bar{P}}\bar{P}^{-1})\zeta + \bar{P}B_p\mathbf{p} \\ \hat{\mathbf{p}} = C\bar{P}^{-1}\zeta. \end{cases} \quad (24)$$

Using the relations

$$\bar{P}A\bar{P}^{-1} = \begin{bmatrix} -K_1 & I \\ -K_2 & 0 \end{bmatrix}$$

and

$$\dot{\bar{P}}\bar{P}^{-1} = \begin{bmatrix} 0 & 0 \\ 0 & \mathcal{RS}(\omega)\mathcal{R}^{-1} \end{bmatrix}$$

$$= \begin{bmatrix} 0 & 0 \\ 0 & S(\mathcal{R}\omega) \end{bmatrix} = \begin{bmatrix} 0 & 0 \\ 0 & S(\omega_r) \end{bmatrix}$$

(24) can be written as

$$\dot{\zeta} = \begin{bmatrix} -K_1 & I \\ -K_2 & S(\omega_r) \end{bmatrix} \zeta + \begin{bmatrix} K_1 \\ K_2 \end{bmatrix} \mathbf{p} \quad (25)$$

$$\hat{\mathbf{p}} = [I \quad 0]\zeta.$$

Simple algebra now shows that $(\mathcal{F}_p - I)W_{\omega_c}^n$ admits the state-space representation

$$(\mathcal{F}_p - I)W_{\omega_c}^n := \left[\begin{array}{c|c} \begin{bmatrix} -K_1 & I & K_1 C_w & 0 \\ -K_2 & S_r & K_2 C_w & 0 \\ 0 & 0 & A_w & B_w \\ I & 0 & -C_w & 0 \end{bmatrix} & \\ \hline \begin{bmatrix} F + KH & KC_w & 0 \\ 0 & A_w & B_w \\ H & -C_w & 0 \end{bmatrix} & \\ \hline \text{Co} \left\{ \begin{bmatrix} F_i + KH & KC_w & 0 \\ 0 & A_w & B_w \\ H & -C_w & 0 \end{bmatrix}, i = \{1, \dots, 8\} \right\} & \end{array} \right] \quad (26)$$

where

$$K = \begin{bmatrix} K_1 \\ K_2 \end{bmatrix}$$

and F , H , and F_i are defined above.

Suppose $\exists P > 0$ and K such that

$$\left[\begin{array}{c|c} P \left[\begin{array}{cc} F_i + KH & KC_w \\ 0 & A_w \end{array} \right] + \left[\begin{array}{cc} F_i + KH & KC_w \\ 0 & A_w \end{array} \right]^T P & P \begin{bmatrix} 0 \\ B_w \end{bmatrix} \\ \hline \left[\begin{array}{cc} H^T \\ -C_w^T \end{array} \right] [H \quad -C_w] & \\ \hline [0 \quad B_w^T] P & -\epsilon^2 I \end{array} \right] < 0,$$

$$i = \{1, \dots, 8\}. \quad (27)$$

Then, using standard results on polytopic system analysis (see [3, eqn. (6.54)]) it follows that $\|(\mathcal{F}_p - I) \cdot W_{\omega_r}^n\| < \epsilon$. Clearly, if the inequalities (27) are satisfied then the gains

$$\begin{bmatrix} K_1 \\ K_2 \end{bmatrix} := K \quad (28)$$

guarantee that $\|(\mathcal{F}_p - I)W_{\omega_r}^n\| < \epsilon$. Notice if expression (27) is satisfied for some \hat{P} and K then the matrices

$$\begin{bmatrix} F_i + KH & KC_w \\ 0 & A_w \end{bmatrix}$$

are stable $\forall i = \{1, \dots, 8\}$ and therefore the polytopic system (25) with state matrix $F + KH$ is internally stable [3]. Since Lyapunov transformations preserve internal stability, the original system (18) is also internally stable.

The above theorem establishes sufficient conditions for the existence of fixed gains K_1 and K_2 such that the complementary filter (18) is internally stable and meets desired frequency-like response characteristics. However, it does not provide any results on the feasibility of the problem at hand. The theorem that follows addresses this problem partially, by showing that there always exists a set of fixed gains for which the filter (18) is internally stable.

THEOREM 3 *Consider the linear time-varying filter (18). Then, for every set of finite positive numbers p_r^+ , q_r^+ , and r_r^+ such that the bounds (22) on ω_r apply there exist fixed gains K_1 and K_2 that make the filter internally stable.*

PROOF From the proof of Theorem 2, the filter (18) is internally stable if and only if the unforced polytopic system

$$\dot{\zeta} = (F + KH)\zeta \quad (29)$$

is internally stable for some choice of K . Given (29), consider the related time-invariant system

$$\dot{\zeta} = (A + KH)\zeta = A_K \zeta \quad (30)$$

where

$$A_K = A + KH; \quad A = \begin{bmatrix} 0 & I \\ 0 & 0 \end{bmatrix}.$$

The simple structures of the matrices A and H implies that (30) can be made stable by choosing $K_1 = k_1 I$, $K_2 = k_2 I$, where k_1 and $k_2 > 0$ are positive but otherwise arbitrary. This stems from the fact that the closed-loop eigenvalues of $A + KH$ have multiplicity three and are easily obtained from the roots of the second-order polynomial $s^2 + k_1 s + k_2$. Therefore, from basic Lyapunov stability theory it follows that for every $\gamma_1 > 0$, $\gamma_2 > 0$ there exists a positive definite matrix

$$P_1 = \begin{bmatrix} P_{11} & P_{12} \\ P_{12} & P_{22} \end{bmatrix} > 0$$

such that

$$A_K^T P_1 + P_1 A_K = -Q = \begin{bmatrix} -\gamma_1 I & 0 \\ 0 & -\gamma_2 I \end{bmatrix}. \quad (31)$$

Expanding (31) we obtain

$$\begin{bmatrix} -2P_{11}K_1 - 2P_{12}K_2 & -P_{12}K_1 - P_{22}K_2 + P_{11} \\ (-P_{12}K_1 - P_{22}K_2 + P_{11})^T & 2P_{12} \end{bmatrix} = \begin{bmatrix} -\gamma_1 I & 0 \\ 0 & -\gamma_2 I \end{bmatrix} \quad (32)$$

and therefore $P_{12} = -(\gamma_2/2)I$. Furthermore, since K_1 and K_2 are diagonal, P_{11} and P_{22} are also diagonal. Consider now the LTI systems

$$\dot{\zeta} = (F_i + KH)\zeta = A_{K_i} \zeta; \quad i = 1, 2, \dots, 8 \quad (33)$$

with F_i defined as before. Using the relation $(S_r^i)^T = -S_r^i$ it follows that

$$A_{K_i} P_1 + P_1 A_{K_i} = \begin{bmatrix} -\gamma_1 I & P_{12} S_r^i \\ (S_r^i)^T P_{12} & -\gamma_2 I \end{bmatrix}; \quad i = 1, 2, \dots, 8. \quad (34)$$

We now show that (34) can be made negative definite for all $i = 1, 2, \dots, 8$ by suitable choice of γ_1 and γ_2 . In fact, using Schur complements [3] it is easily shown that (34) is negative definite if and only if

$$\gamma_1 I - P_{12} S_r^i \gamma_2^{-1} (S_r^i)^T P_{12} = \gamma_1 I - (\gamma_2/4) S_r^i (S_r^i)^T > 0.$$

Since $\|S_r^i(\omega_r^i)\| = \|\omega_r^i\|$, the above expression is satisfied with $\gamma_2 = 4$ and $\gamma_1 > \max\{\|\omega_r^i\|^2 : i = 1, 2, \dots, 8\}$. Hence, using the theory of polytopic systems [3] the system (29) and therefore the original complementary filter are internally stable.

Note: From the proof of the theorem, it follows that the linear time-varying filter (18) is internally stable for any choice of constant, positive, diagonal matrices K_1 and K_2 .

We now address the issue of performance robustness of the complementary filter in the presence of measurement errors in the rotation matrix \mathcal{R} . In what follows, we let $\mathcal{R} = \mathcal{R}(\lambda)$ and $\mathcal{R}_m = \mathcal{R}_m(\lambda_m)$ denote the ‘‘true’’ and measured rotation matrices, which are functions of the ‘‘true’’ and measured orientation vectors λ and λ_m , respectively. We further let $\mathcal{R} - \mathcal{R}_m = \Delta\mathcal{R}$ and assume that $\Delta\mathcal{R}$ is bounded, that is, there exists a positive constant δ_R such that $\|\Delta\mathcal{R}\| \leq \delta_R$.

To compute the influence of $\Delta\mathcal{R}$ on the estimation error $\mathbf{e}_p = \mathbf{p} - \hat{\mathbf{p}}$, we set $\mathbf{p}_m = \mathbf{p}$ and $\mathbf{v}_m = \mathbf{v}$. From (14) and (18) it follows that the error \mathbf{e}_p is the output of a dynamical system with input \mathbf{v} and state space realization

$$\mathcal{F}_e := \begin{bmatrix} -K_1 & \mathcal{R}_m & \Delta\mathcal{R} \\ -\mathcal{R}_m^{-1} K_2 & 0 & 0 \\ I & 0 & 0 \end{bmatrix}. \quad (35)$$

The state matrix of \mathcal{F}_e equals that of \mathcal{F} in Theorem 1. Therefore, internal stability is obtained if the conditions of Theorem 2 are met with \mathcal{R} replaced by \mathcal{R}_m . In particular, if the filter gains K_1 and K_2 are constant, diagonal, and positive then internal stability is automatically ensured (see Theorem 3). The issue of robust performance requires further thought, but can be addressed by viewing \mathcal{F}_e as an input-output operator with realization

$$\overline{\mathcal{F}}_e := \left[\begin{array}{cc|c} -K_1 & \mathcal{R}_m & I \\ \hline -\mathcal{R}_m^{-1}K_2 & 0 & 0 \\ \hline I & 0 & 0 \end{array} \right] \quad (36)$$

and input $\mathbf{u} = \Delta\mathcal{R}\mathbf{v}$. If \mathbf{v} is bounded uniformly in time, that is, $\|\mathbf{v}\|_\infty = \mathbf{v}_\infty < \infty$ then

$$\|\mathbf{u}\|_\infty \leq \|\Delta\mathcal{R}\| \|\mathbf{v}\|_\infty = \delta_R \mathbf{v}_\infty.$$

Since $\overline{\mathcal{F}}_e$ is internally stable, the induced norm $\|\overline{\mathcal{F}}_e\|_{\infty,i}$ of the corresponding operator is finite. Therefore,

$$\|\mathbf{e}(t)\|_2 \leq \|\mathbf{e}\|_\infty \leq \|\overline{\mathcal{F}}_e\|_{\infty,i} \delta_R \mathbf{v}_\infty$$

for all t in \mathcal{R}_+ . Thus, the estimation error $\mathbf{e}(t)$ remains bounded for all t in the presence of measurement errors in \mathcal{R} and decreases uniformly to zero as δ_R approaches zero.

From the discussion above, it follows that the induced operator norm $\|\overline{\mathcal{F}}_e\|_{\infty,i}$ is the correct measure of performance robustness of the filter against measurement perturbations in the rotation matrix \mathcal{R} . A constraint on $\|\overline{\mathcal{F}}_e\|_{\infty,i}$ can be included in the filter design process by using the circle of ideas discussed in [20].

VI. FILTER DESIGN: A PRACTICAL ALGORITHM. SIMULATION RESULTS

The previous section introduced the mathematical tools that are required to design a candidate complementary filter with a guaranteed break frequency. Notice, however, that the outcome of the design process may very well be a filter with an effective bandwidth that is greater than the one required. Clearly, the set of possible solutions must be further constrained so that the designer have an extra design parameter at his disposal to select one solution (if it exists) that meets the required break frequency criterion. This situation is identical to what happens in the case of filter design using Kalman–Bucy theory, where the noise covariances play the role of tuning knobs to shape the filter characteristics.

In the LTI case, a simple analysis of a Bode diagram indicates that an expedite way of setting an upper bound on the break frequency is to make the filter roll-off sufficiently fast. In the time-varying setting, this corresponds to making $\|\mathcal{F}_p \mathcal{W}_{\omega_i}^{n_i}\| < \gamma$, where $\mathcal{W}_{\omega_i}^{n_i}$ is a high pass Chebyshev filter and ω_i and

γ play the role of “tuning parameters.” In practice, it is sufficient to vary the value of the parameter γ .

These considerations lead directly to a *practical algorithm* for the *design* of a time-varying complementary filter with a desired break frequency ω_c . This is done by using Theorem 1 with the additional “high-frequency” constraint described above, which can be also cast as an LMI. The underlying optimization problem can be formulated as follows:

$$\begin{aligned} & \min_K \gamma \\ & \text{subject to} \\ & \|(I - \mathcal{F}_p) \mathcal{W}_{\omega_c}^{n_i}\| < \epsilon_0 \\ & \|\mathcal{F}_p \mathcal{W}_{\omega_i}^{n_i}\| < \gamma \end{aligned} \quad (37)$$

where the minimization is performed over the the set of gain matrices $K \in \mathcal{R}^{6 \times 3}$ and ϵ_0 captures the low pass requirement constraint. It is simple to see that the high pass constraint $\|\mathcal{F}_p \mathcal{W}_{\omega_i}^{n_i}\| < \gamma$ is satisfied if $\exists Y > 0$ and K such that

$$L_{HP_i}(Y, K, \gamma) := \left[\begin{array}{cc|c} Y \left[\begin{array}{cc} F_i + KH & KC_{W_i} \\ 0 & A_{W_i} \end{array} \right] + \left[\begin{array}{cc} F_i + KH & KC_{W_i} \\ 0 & A_{W_i} \end{array} \right]^T Y & Y \left[\begin{array}{c} KD_{W_i} \\ B_{W_i} \end{array} \right] \\ \hline + \left[\begin{array}{c} H^T \\ 0 \end{array} \right] \left[\begin{array}{cc} H & 0 \end{array} \right] & \\ \hline \left[\begin{array}{cc} KD_{W_i} & B_{W_i}^T \end{array} \right] Y & \left[\begin{array}{c} -\gamma^2 I \end{array} \right] \end{array} \right] < 0, \quad i = \{1, \dots, 8\} \quad (38)$$

where

$$\mathcal{W}_{\omega_i}^{n_i} = \begin{bmatrix} A_{W_i} & B_{W_i} \\ C_{W_i} & D_{W_i} \end{bmatrix}.$$

The optimization problem (37) can now be cast in the LMI framework as follows. For given numbers $\epsilon > 0$ and $\gamma > 0$ define the sets

$$\Phi_{LP}(\epsilon) = \{K, P : P > 0, L_{LP_i}(K, P, \epsilon) < 0, \quad \forall i = \{1, \dots, 8\}\} \quad (39)$$

$$\Phi_{HP}(\gamma) = \{K, Y : Y > 0, L_{HP_j}(K, Y, \gamma) < 0, \quad \forall j = \{1, \dots, 8\}\} \quad (40)$$

where the expressions $L_{LP_i}(K, P, \epsilon)$ and $L_{HP_j}(K, Y, \gamma)$ were defined in (23) and (38), respectively. Then the solution K to the optimization problem (37) can be obtained by solving the following constrained optimization problem:

$$\min_{(K,P) \in \Phi_{LP}(\epsilon_0); (K,Y) \in \Phi_{HP}(\gamma)} \gamma. \quad (41)$$

The optimization problem (41) is nonconvex. However, the matrix inequalities $L_{LP_i}(K, P, \epsilon) < 0$ and $L_{HP_j}(K, Y, \gamma) < 0$ are jointly linear in the parameters

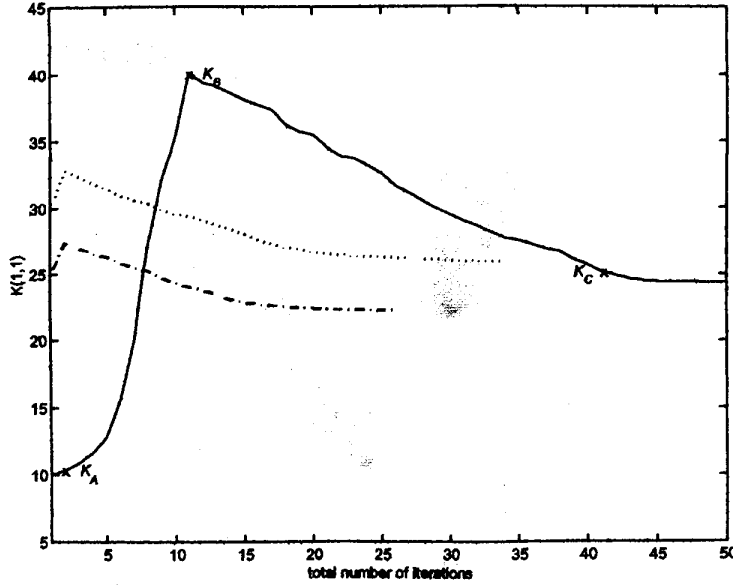


Fig. 6. Filter gain $K(1,1)$ versus iteration number.

P , K , and Y . Therefore, for fixed K the expressions $L_{LR}(K, P, \epsilon)$ and $L_{HP}(K, Y, \gamma)$ are linear in P and Y , respectively, and for fixed P and Y they are linear in K . This observation suggests the following numerical solution/design procedure to solve the above constrained optimization problem (see [9] and references therein for similar approaches reported in the literature).

I. Initialization

1. Fix $\epsilon > \epsilon_0 > 0$. From operational conditions, determine the operating range of angular velocities p_r, q_r, r_r :

$$|p_r| \leq p_r^+, \quad |q_r| \leq q_r^+, \quad |r_r| \leq r_r^+.$$

2. Specify the frequency ω_c and use it to construct the low pass weight $\mathcal{W}_{\omega_c}^n$.

3. Specify the bandwidth ω_l of the high-pass weight $\mathcal{W}_{\omega_l}^n$. (As a rule-of-thumb choose $\omega_l \gg \omega_c$).

4. Select initial values for the gains K_1, K_2 . (As suggested by Theorem 3 any gains of the form $\gamma_1 I, \gamma_2 I, \gamma_1 > 0, \gamma_2 > 0$ will do.)

II. Numerical Optimization

1. Low pass constraint. Solve

$$\min_{(P,K) \in \Phi_{LP}(\epsilon), \epsilon \geq \epsilon_0} \epsilon. \quad (42)$$

Use $K = [\gamma_1^T \ \gamma_2^T]^T$ obtained in step I.4 to initialize K , then iterate over P and K to solve the optimization problem (42). If no solution is found, increase ϵ_0 .

2. High pass constraint. Let (P^*, K^*) denote the solution to the optimization problem (42). Solve

$$\min_{(Y,K) \in \Phi_{HP}(\gamma), (P^*, K) \in \Phi_{LP}(\epsilon_0)} \gamma. \quad (43)$$

Use K^* as an initial value for K , then iterate over Y and K to solve the optimization problem (43).

Due to nonconvexity the numerical solutions proposed in Steps II.1 and II.2 are not guaranteed to converge to a local minimum [9]. Therefore, the algorithm should be run for multiple initial conditions. It is then up to the system designer to select appropriate values of the tuning parameters to try and meet all the criteria that must be satisfied by a complementary filter with a desired break frequency. See the definitions of *complementary filter with break frequency* ω_c and *low pass filter with bandwidth* ω_c introduced earlier.

To illustrate the performance of the complementary filtering structure, a simple filter design exercise was carried out for an autonomous surface vehicle undergoing rotational maneuvers in the horizontal plane. In this case, the navigation system is required to provide accurate estimates of the vehicle's position based on position and velocity measurements provided by a DGPS and a Doppler sonar, respectively. In the scenario adopted, the vehicle progresses at a constant speed of 2 m/s while it executes repeated turns at a maximum yaw rate of 3 rad/s. The Doppler sonar is assumed to introduce a constant bias term $v_{d,0} = [0.1 \text{ m/s}, 0.2 \text{ m/s}]^T$. The selected break frequency for the complementary filter was $\omega_c = 0.4$ rad/s.

The design procedure is illustrated in Figs. 6–8. In the design, the orders n and n_l of the Chebyshev weights $\mathcal{W}_{\omega_c}^n$ and $\mathcal{W}_{\omega_l}^{n_l}$ were selected as 2. Furthermore, ω_l was set arbitrarily to 60 rad/s. The performance parameter ϵ_0 for the low pass filter was chosen as 0.2.

Fig. 6 shows the evolution of the complementary filter gain $K(1,1)$ for three different initial values. The bold curve shows clearly the general tendency for the case where the initial values are small: the filter

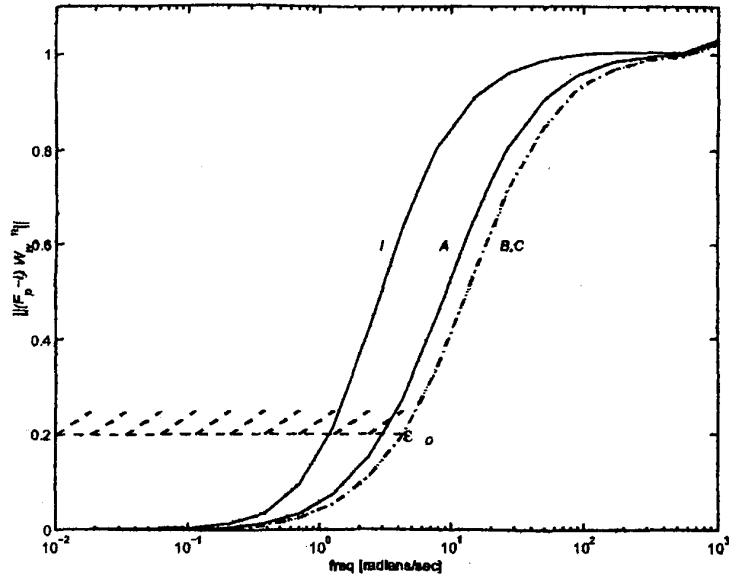


Fig. 7. Generalized Bode plots. Low pass property.

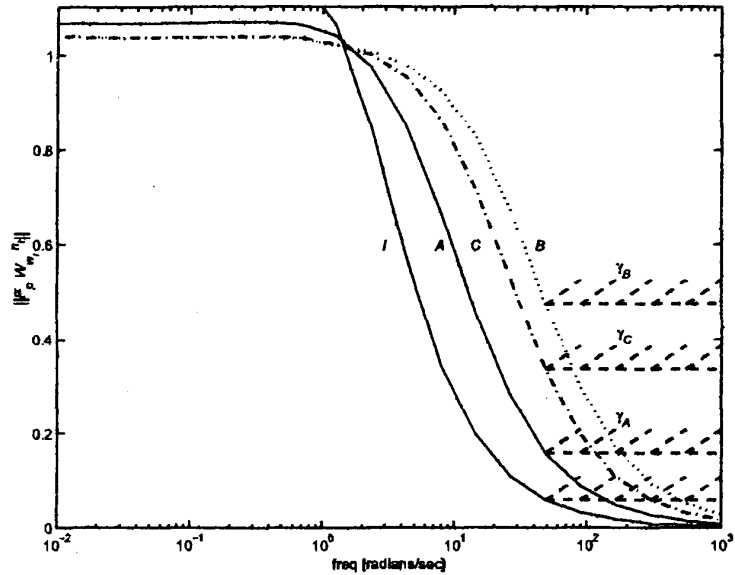


Fig. 8. Generalized Bode plots. High pass property.

does not exhibit a high enough break frequency, and therefore the gains are increased until the low pass requirement is met, possibly with a certain margin (the margin depends on the particular sequence of iterations obtained by running the first minimization problem in (42)). At this point, the high pass constraint comes into play, forcing the gains to change until the low pass constraint is met, without incurring too much spillover at high frequencies.

The three lower curves in Fig. 7 are plots of $\|(\mathcal{F}_p - I)\mathcal{W}_{\omega_c}^n\|$ as a function of ω_c , the operator \mathcal{F}_p being computed with the gains obtained at steps A, B, and C of Fig. 6. The top curve I shows the case

where the filter gains were set to values much smaller than those obtained in step A. Henceforth, we refer to such plots as *generalized Bode plots*. The figure shows clearly that the filter starts with a break frequency that is smaller than that required, that frequency being increased until the break frequency requirement is met. It is the role of the high pass constraint to guarantee that the low pass requirement be met while reducing the spillover at high frequencies. Fig. 8 shows the evolution of $\|(\mathcal{F}_p)\mathcal{W}_{\omega_c}^n\|$ as a function of ω_c . The iterative procedure described above aims at minimizing the value γ of these generalized Bode plots at $\omega = 60$ rad/s subject to the low pass constraint

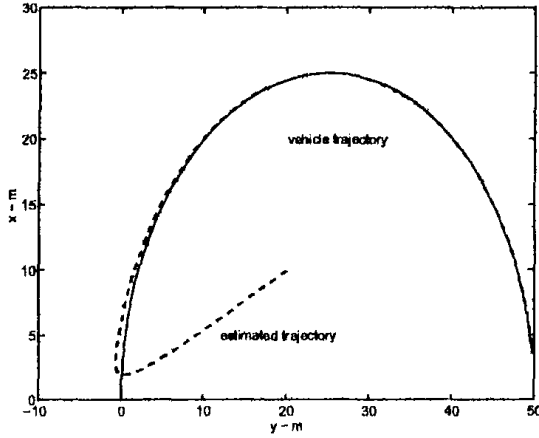


Fig. 9. Actual and estimated vehicle trajectory.

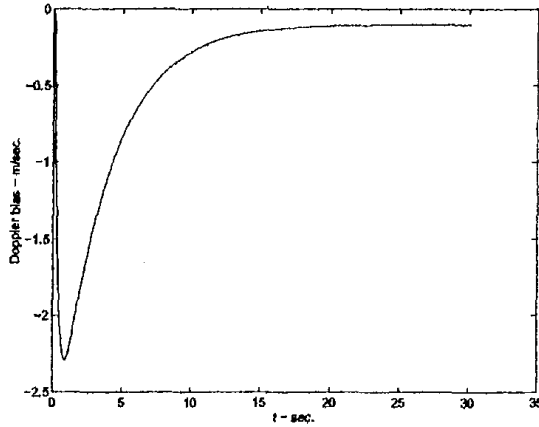


Fig. 10. Doppler bias estimate.

described before. The cases *I* and *A* violate the low pass constraint and are therefore not important to examine. Notice, however, how the value of γ decreases from iteration *B* to *C*, thus showing that in case *C* less spillover is introduced at high frequency.

The performance of the resulting filter was assessed in simulation. Fig. 9 shows the actual and estimated vehicle position when the initial state of the filter was set to $\mathbf{x}_1 = [10 \text{ m}, 20 \text{ m}]^T$ and $\mathbf{x}_2 = [0 \text{ m/s}, 0 \text{ m/s}]^T$. Fig. 10 captures the evolution of the first component of the Doppler bias estimate. It can be concluded from the figures that the filter provides good tracking of the actual inertial trajectory and rejects the bias introduced by the Doppler unit in the body-axis.

VII. EXTENSION TO ACCELEROMETERS

In this section we extend the results discussed above to include the case of complementing position information with that available from onboard accelerometers. This is a scenario commonly

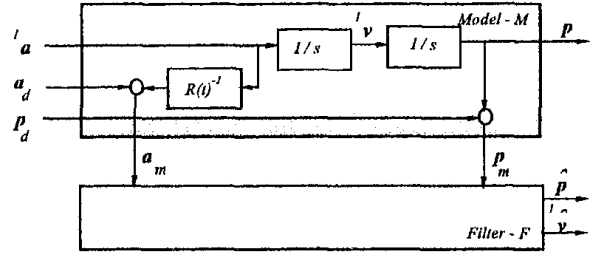


Fig. 11. Process model \mathcal{M}_{pa} .

encountered in the case of air vehicles. First, we introduce additional notation.

- ${}^I \mathbf{a}$ Linear acceleration of the origin of $\{\mathcal{B}\}$ measured in $\{\mathcal{I}\}$.
- \mathbf{a} Linear acceleration of the origin of $\{\mathcal{B}\}$ with respect to $\{\mathcal{I}\}$, resolved in $\{\mathcal{B}\}$.

Using this notation we establish the following kinematic relationships for the case of accelerometers:

$$\dot{\mathbf{p}} = {}^I \mathbf{v} \quad (44)$$

$${}^I \dot{\mathbf{v}} = {}^I \mathbf{a} = \mathcal{R} \mathbf{a} \quad (45)$$

$$\dot{\mathcal{R}} = \mathcal{R} S(\boldsymbol{\omega}). \quad (46)$$

The underlying process model \mathcal{M}_{pa} is depicted in Fig. 11, where \mathcal{F} is a dynamical system (filter) that operates on the measurements \mathbf{p}_m and \mathbf{a}_m to provide estimates $\hat{\mathbf{p}}$ of \mathbf{p} . In the figure, \mathbf{p}_d and \mathbf{a}_d are measurement disturbances. As in Section V, we study the situation where $\mathbf{p}_d = 0$ and $\mathbf{a}_d = \mathbf{a}_{d,0}$ where $\mathbf{a}_{d,0}$ is the accelerometer bias.

DEFINITION Process Model \mathcal{M}_{pa} . The process model \mathcal{M}_{pa} is given by

$$\mathcal{M}_{pa} := \begin{cases} \dot{\mathbf{p}} = {}^I \mathbf{v} \\ {}^I \dot{\mathbf{v}} = {}^I \mathbf{a} \\ \mathbf{p}_m = \mathbf{p} \\ \mathbf{a}_m = \mathcal{R}^{-1} \mathbf{a} + \mathbf{a}_{d,0}. \end{cases} \quad (47)$$

The discussion in the previous sections leads directly to the following filter design problem.

Problem Formulation. Given the process model \mathcal{M}_{pa} in (47) and positive numbers ω_c , n , and c , find an (ϵ, n) complementary filter for \mathcal{M}_{pa} with break frequency ω_c .

The theorem that follows introduces a candidate complementary filter for \mathcal{M}_{pa} (see Fig. 12). The filter structure is motivated by the results presented in previous sections, where an extra integrator was inserted to estimate the Doppler bias.

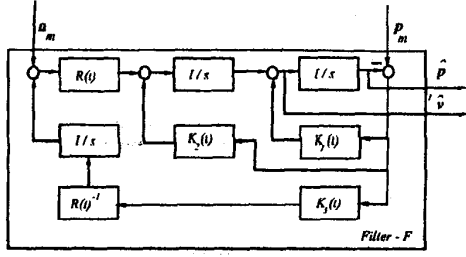


Fig. 12. Complementary filter \mathcal{F}_a .

THEOREM 4 Consider the process model M_{pa} and the time-varying filter

$$\mathcal{F} := \begin{cases} \dot{\mathbf{x}}_1 = \mathbf{x}_2 + K_1(\mathbf{p} - \mathbf{x}_1) \\ \dot{\mathbf{x}}_2 = R\mathbf{a}_m + R\mathbf{x}_3 + K_2(\mathbf{p} - \mathbf{x}_1) \\ \dot{\mathbf{x}}_3 = R^{-1}K_3(\mathbf{p} - \mathbf{x}_1) \\ \hat{\mathbf{p}} = \mathbf{x}_1. \end{cases} \quad (48)$$

Suppose the filter \mathcal{F} is internally stable. Then, \mathcal{F} is a candidate complementary filter for M_{pa} .

The next result establishes sufficient conditions for the existence of fixed gains K_1 , K_2 , and K_3 such that the candidate filter is internally stable and has a guaranteed break frequency of at least ω_c , where ω_c is a design parameter.

THEOREM 5 Consider the linear time-varying filter (48) and assume that the bounds (22) on ω_r apply. Given n and ω_c , let $W_{\omega_c}^n$ be given by Theorem 2. Further let

$$F = \begin{bmatrix} 0 & I & 0 \\ 0 & 0 & I \\ 0 & 0 & S_r \end{bmatrix}, \quad H = [I \ 0 \ 0].$$

Suppose that given $\epsilon > 0 \exists K \in \mathcal{R}^{9 \times 3}$, $P \in \mathcal{R}^{(9+n) \times (9+n)}$, $P > 0$ such that the LMIs

$$\left[\begin{array}{c|c} P \left[\begin{array}{cc} F_i + KH & KC_w \\ 0 & A_w \end{array} \right] + \left[\begin{array}{cc} F_i + KH & KC_w \\ 0 & A_w \end{array} \right]^T P & P \begin{bmatrix} 0 \\ B_w \end{bmatrix} \\ \hline \left[\begin{array}{c} H^T \\ -C_w^T \end{array} \right] [H \ -C_w] & -\epsilon^2 I \end{array} \right] < 0, \quad (49)$$

$$F_i = \begin{bmatrix} 0 & I & 0 \\ 0 & 0 & I \\ 0 & 0 & S(\omega^i) \end{bmatrix}, \quad i = \{1, \dots, 8\}$$

are satisfied. Then, the constant gains

$$\begin{bmatrix} K_1 \\ K_2 \\ K_3 \end{bmatrix} := K$$

make the filter \mathcal{F} internally stable. Furthermore, the operator $\mathcal{F}_p : \mathbf{p} \rightarrow \hat{\mathbf{p}}$ satisfies a low pass property with indices (ϵ, n) over $[0, \omega_c]$, that is, $\|(\mathcal{F}_p - I)W_{\omega_c}^n\| < \epsilon$.

The proofs of Theorems 4 and 5 follow directly from the proofs of Theorems 1 and 2 and can also be found in [14]. The robustness of the filter \mathcal{F} with respect to uncertainties in the rotation matrix $R(t)$ can be analyzed using the steps outlined in Section V. Similarly, the filter design procedure given in Section V applies to the design of filter (48).

VIII. IMPLEMENTATION ISSUES

The complementary filter presented in Section IVB can be used to estimate position and velocity of an ocean surface or underwater vehicles. In the case of a surface vehicles the position information can be obtained from DGPS, while velocity information can be provided by a Doppler sonar. (For an excellent reference on Doppler sonar we refer the reader to [15]). In the case of a fully submerged underwater vehicle the position information can be provided by the Long Baseline System.

Similarly, for the case of the complementary filter in Section VII the position information can be obtained from DGPS, while accelerations are available from the Inertial Measurement Unit. In all cases the rotation matrix \mathcal{R} can be computed using the Attitude and Heading Reference System (AHRS), see [15].

IX. CONCLUSIONS

This paper extended the theory of complementary filtering to the time-varying setting. In particular, the frequency domain interpretations of complementary filters were extended by resorting to the theory of linear differential inclusions and by converting the problem of weighted filter performance analysis into that of determining the feasibility of a related set of LMIs. Using this set-up, it has been shown how the stability of the resulting filters as well as their frequency-like performance can be assessed using efficient numerical analysis tools that borrow from convex optimization techniques. The cases of complementing position information with that available from onboard Doppler sonar and accelerometers have been considered. The resulting design methodology was successfully applied to a design example. Future work will aim at extending these results to the discrete-time, multirate case.

REFERENCES

- [1] Bar-Itzhack, I., and Ziv, I. (1986) Frequency and time domain designs of strapdown vertical determination systems. In *Proceedings of AIAA Guidance, Navigation and Control*, Williamsburgh, PA, Aug. 1986, 505–515.
- [2] Becker, G., and Packard, A. (1993) Robust performance of linear, parametrically varying systems using parametrically-dependent linear, dynamic feedback. *Systems and Control Letters*, 1993.

- [3] Boyd, S., El Ghaoui, L., Feron, E., and Balakrishnan, B. (1994)
Linear Matrix Inequalities in Systems and Control Theory. Philadelphia: (SIAM Studies in Applied Mathematics), 1994.
- [4] Britting, K. (1971)
Inertial Navigation System Analysis. New York: Wiley-Interscience, 1971.
- [5] Brockett, R. (1992)
Finite Dimension Linear Systems. New York: Wiley, 1992.
- [6] Brown, R., and Hwang, P. (1992)
Introduction to Random Signals and Applied Kalman Filtering (2nd ed.). New York: Wiley, 1992.
- [7] Brown, R. (1972)
Integrated navigation systems and Kalman filtering: A perspective.
Journal of the Institute of Navigation, **19**, 4 (Winter 1972–1973), 355–362.
- [8] Fryxell, D., Oliveira, P., Pascoal, A., and Silvestre, C. (1994)
An integrated approach to the design and analysis of navigation, guidance and control systems for AUVs.
In *Proceedings of the Symposium on Autonomous Underwater Vehicle Technology*, Cambridge, MA, 1994.
- [9] Goh, K. C., Turan, L., Safonov, M. G., Papavassilopoulos, G. P., and Ly, J. H. (1994)
Biaffine matrix inequality properties and computational methods.
In *Proceedings of the 1994 American Control Conference*, Baltimore, MD, 1994, 850–855.
- [10] Goodwin, G., and Seron, M. (1997)
Fundamental design tradeoffs in filtering, prediction, and smoothing.
IEEE Transactions on Automatic Control, **42**, 9 (Sept. 1997), 1240–1251.
- [11] Green, M., and Limebeer, D. (1995)
Linear Robust Control. Englewood Cliffs, NJ: Prentice-Hall, 1995.
- [12] Grigoriadis, K., and Watson, J. (1997)
Reduced-order H_∞ and $L_2 - L_\infty$ filtering via linear matrix inequalities.
IEEE Transactions on Aerospace and Electronic Systems, **33**, 4 (Oct. 1997), 1326–1338.
- [13] Jourdan, D. (1985)
Doppler sonar navigation error propagation and correction.
Journal of the Institute of Navigation, **32**, 1 (Spring 1985), 29–56.
- [14] Kammer, L., and Pascoal, A. M. (1998)
Navigation system design using time-varying complementary filters.
Internal report, Naval Postgraduate School, Jan. 1998.
- [15] Kayton, M., and Fried, W. (Ed.) (1996)
Avionics Navigation Systems. New York: Wiley, 1996.
- [16] Lin, C. (1991)
Modern Navigation, Guidance, and Control Processing. Englewood Cliffs, NJ: Prentice-Hall, 1991.
- [17] The Math Works Inc. (1997)
MatLab Application Toolbox, LMI Control.
- [18] Merhav, S. (1996)
Aerospace Sensor Systems and Applications. New York: Springer-Verlag, 1996.
- [19] Nagpal, K., and Khargonekar, P. (1991)
Filtering and smoothing in an H_∞ setting.
IEEE Transactions on Automatic Control, **36** (1991), 152–166.
- [20] Scherer, C., Gahinet, P., and Chilali, M. (1997)
Multiobjective output-feedback control via LMI optimization.
IEEE Transactions on Automatic Control, **42**, 7 (July 1997), 896–911.
- [21] Siouris, G. (1993)
Aerospace Avionics Systems: A Modern Synthesis. New York: Academic Press, 1993.
- [22] Stambaugh, J., and Thibault, R. (1992)
Navigation requirements for autonomous underwater vehicles.
Journal of the Institute of Navigation, **39**, 1 (Spring 1992), 79–92.
- [23] Vidyasagar, M. (1985)
Control System Synthesis: A Factorization Approach. Cambridge, MA: MIT Press, 1985.
- [24] Youngberg, J. (1991)
A novel method for extending GPS to underwater vehicles.
Journal of the Institute of Navigation, **38**, 3 (Fall 1991), 263–271.

António M. Pascoal received the Ph.D. degree in control science from the University of Minnesota, Minneapolis.

From 1978–1988 he was a research scientist with Integrated Systems Incorporated, Santa Clara, CA. From 1988–1993 he was an Assistant Professor with the Department of Electrical Engineering of the Instituto Superior Técnico (IST), Lisbon, Portugal, where he is currently an Associate Professor of Control and Robotics. In 1993 he joined the Institute for Systems and Robotics of IST, where he is the Coordinator of the Dynamical Systems and Ocean Robotics Laboratory. In 1997 he was a Visiting Associate Professor with the Department of Aeronautics and Astronautics and the Department of Mechanical Engineering of the U.S. Naval Postgraduate School of Monterey, CA. Since January 1998, he has been the leader of a European team that is developing advanced systems for the coordinated operation of robotic ocean vehicles with applications to the study of hydrothermal vent activity in the Azores islands. His research interests include navigation, guidance, and control theory, combined plant/controller optimization, nonlinear control, and advanced mission control systems with applications to robotic air and ocean vehicles.



Isaac Kaminer obtained the M.S.E. degree from the University of Minnesota, Minneapolis, in 1985. He received the Ph.D. degree from the University of Michigan, Ann Arbor, in 1992.

He worked for the Boeing Company between his M.S.E. degree and Ph.D. degree, first on 757/767 program and then in the guidance and control research group. He is currently an associate professor at the Department of Aeronautics and Astronautics at the Naval Postgraduate School, Monterey, CA. He has been a faculty member at the Aero Department since August of 1992. His research interests include integrated plant-controller optimization and integrated guidance, navigation and control of UAVs.



Paulo Oliveira received his Licenciatura and M.Sc. degrees in electrical engineering from the Instituto Superior Técnico (IST), Lisbon, Portugal in 1987 and 1991, respectively.

Since 1989, he has been a Teaching Assistant of Control and Robotics at the Department of Electrical Engineering of IST. In 1993, he joined the staff of the Institute for Systems and Robotics (ISR) at IST. Over the past years, he has participated actively in the design, development and testing of vehicle and mission control systems for underwater robots. He is currently pursuing a Ph.D. degree in the area of underwater vehicle navigation. His research interests are in the areas of navigation, multirate systems, and mission control systems with applications to underwater vehicles.

